AMERICAN SOCIETY of
GENE & CELL
THERAPY

Targeting Lymph Node Sinus Macrophages to Inhibit Lymph Node Metastasis

Junqing Hu,[1] Jinhao Xu,[1] Mingyue Li,[1] Yanping Zhang,[1] Huaiqiang Yi,[1] Jiangning Chen,[1] Lei Dong,[1] Junfeng Zhang,[1] and Zhen Huang[1]

[1]State Key Laboratory of Analytical Chemistry for Life Sciences and Collaborative Innovation Center of Chemistry for Life Sciences, State Key Laboratory of Pharmaceutical Biotechnology, School of Life Sciences, Nanjing University, Nanjing 210023, P.R. China

Lymph nodes are important peripheral immune organs in which numerous important immune responses occur. During the process of lymphatic metastasis, lymph nodes are also sites through which tumor cells must pass. Therefore, it is essential to develop a drug delivery system that can specifically transfer immunostimulatory medicine into lymph nodes to block lymphatic metastasis. Here, we developed a nucleic acid drug delivery system containing cationic agarose (C-agarose) and CpG oligodeoxynucleotides. C-agarose has a high affinity for Siglec-1 on the surface of lymph node sinus macrophages, which have a high specificity for targeting lymph nodes. Subcutaneous implantation of C-agarose+CpG gel caused the accumulation of CpG in the lymph node sinus macrophages and generated antitumor immune responses in the lymph node. C-agarose+CpG gel treatment decreased the metastasis size in the tumor-draining lymph node (TDLN) and lung metastatic nodules and suppressed tumor growth in both a mouse 4T1 breast cancer model and a B16F10 melanoma model. On this basis, this study proposes a nonsurgical invasive lymph node targeting immunotherapy concept that may provide a new approach for antitumor metastasis.

INTRODUCTION

Cancer metastasis, the dissociation of malignant cells from the primary tumor tissue to initiate the growth of a secondary tumor at a distant site, is the main cause of death in cancer patients.[1,2] A lot of clinical data have indicated that lymphatic metastasis is an early event and the primary route of most solid tumor metastasis, including melanoma and breast cancer.[3,4] The existence of tumor cells in the tumor-draining lymph node (TDLN) is important evidence for tumor staging and prognosis.[5,6] Therefore, blocking the spreading of tumor cells via lymphatic vessels may substantially prolong the life cycle of cancer patients. Current strategies for managing lymphatic metastasis include lymph node dissection and radiation therapy, which are accompanied by pain, lymphedema, and joint movement disorders that may influence the life quality of patients, and remaining microscopic metastasis may lead to tumor recurrence.[7,8] Meanwhile, therapeutic reagents such as chemotherapy drugs and biological agents have difficulty accessing the metastatic lymph nodes when administered systemically.[9] Thus, developing novel approaches to target delivery of therapeutic reagents to metastatic lymph nodes may prevent tumor metastasis and, consequently, reduce mortality.

As peripheral lymphoid organs, lymph nodes are filled with immune cells that act as filters to trap germs, viruses, tumor cells, and foreign particles.[5] During the progression of lymphatic metastasis, primary tumors secrete large amounts of immunomodulatory molecules that establish the immunological suppression in TDLNs and provide a favorable environment for tumor cell proliferation.[10,11] Theoretically, strategies based on destroying immunological tolerance and restoring antitumor immunity in lymph nodes can achieve the goal of preventing tumors from spreading via lymphatic vessels.

Lymph node sinus macrophages, localized in the subcapsular sinus (SCS) and medulla of lymph nodes and expressing Siglec-1 (CD169), can present antigens and activate natural killer (NK) cells and cytotoxic T lymphocytes (CTLs).[12–14] Moreover, the density of lymph node Siglec-1^{+} macrophages is positively associated with a good prognosis for patients with various types of cancer.[15–18] Thus, lymph node sinus macrophages play a key role in antitumor immune responses. CpG oligodeoxynucleotides (CpG ODNs) are short single-stranded synthetic DNA molecules that contain unmethylated CpG motifs that can be detected by Toll-like receptor 9 (TLR9) and finally lead to a protective immune response.[19] Therefore, CpG ODNs are currently being evaluated for anticancer immunotherapy.[20] However, prolonged and high-dose systemic administration of free CpG may seriously interfere with the body's immune homeostasis, leading to severe side effects, including immune cell exhaustion, destruction of lymphoid follicles, liver damage, and exacerbation of autoimmune diseases.[21] To reduce these adverse effects, activating immune cell

subsets in specific organs by a drug delivery system containing CpG ODNs should be adopted to ensure an antitumor effect and avoid unwanted interferences with normal physiological functions. In our previous studies, we observed that cationic agarose (C-agarose) hydrogel had a high affinity for lymph node sinus macrophages.[22] Therefore, a nucleic acid drug delivery system based on C-agarose hydrogel and CpG oligonucleotides was used to target lymph node sinus macrophages and reactivate antitumor immune responses in lymph nodes in this study. The inhibitory effect on tumor metastasis was further evaluated in mouse models of breast cancer and melanoma.

RESULTS

Biodistribution of C-agarose+CpG Hydrogel in 4T1 Tumor-Bearing Mice

The levels of CpG in different mouse tissues were examined 1 week after gel implantation. Compared with that resulting from the injection of agarose+CpG, the administration of C-agarose+CpG greatly enhanced the accumulation of CpG in the lymph nodes and spleen and reduced the deposition of nucleic acid in other tissues (Figure 1A). The CpG levels in different types of cells from the lymph node were examined by both immunofluorescence staining and flow cytometry. T cells (CD3^{+}) and its subsets (CD4^{+}, CD8^{+}), B cells (B220^{+}), dendritic cells (CD11c^{+}), and NK cells (CD49b^{+}) were Siglec-1^{−} cells (Figure S1A). As shown in Figures 1B and S1B, C-agarose could specifically deliver CpG into Siglec-1^{+} macrophages rather than Siglec-1^{−} cells. Flow cytometry also indicated that Cy3-CpG accumulated in Siglec-1^{+} macrophages, but not in Siglec-1^{−} cells (Figures 1C and S1C). To further determine the cellular CpG level, Siglec-1^{+} macrophages were purified from the lymph nodes, and other cells during the isolation process were collected and designated as non-Siglec-1^{+} macrophages. Consistent with the immunofluorescence results, CpG was accumulated in Siglec-1^{+} macrophages rather than in non-Siglec-1^{+} macrophages (Figure 1D).

### *In Vitro* Transfection of the C-agarose+CpG Complex

Cy3-labeled CpG was applied to examine the transfection efficiency of C-agarose+CpG in Siglec-1^{+} macrophages. Compared with that of naked CpG-treated cells, C-agarose greatly enhanced the cellular uptake of CpG, and its transfection efficiency was comparable to that of Lipofectamine 2000-treated cells (Figures 1E and 1F). As the Siglec-1 molecule can bind with sialic acid and galactose is an important component of sialic acid, we applied *Siglec-1* small interfering RNA (siRNA) and plasmid encoding Siglec-1 to examine the role of Siglec-1 in the cellular uptake of the C-agarose+CpG complex. Western blot results demonstrated that Siglec-1 expression was reduced in Siglec-1^{+} macrophages treated with *Siglec-1* siRNA (Figure S2A); meanwhile, the transfection of plasmid-encoding Siglec-1 could further increase Siglec-1 expression (Figure S2C). Neither *Siglec-1* siRNA nor Siglec-1 plasmid treatment affected the viability of Siglec-1^{+} macrophages (Figures S2B and S2D). Both the results of microscopical images and the flow cytometer data indicated that *Siglec-1* siRNA pretreatment could reduce the transfection efficiency of C-agarose+CpG complex, and overexpression of Siglec-1 could enhance the cellular uptake of CpG (Figures 1G and 1H). We also

applied a Siglec-1 antibody to block Siglec-1 molecules on the surface of macrophages. However, the blockade of antibody did not significantly reduce the transfection efficiency of C-agarose+CpG complex (Figure S3). It is possible that the binding site of Siglec-1 to the C-agarose+CpG complex could not be fully blocked by the antibody. As either upregulation or downregulation of Siglec-1 could enhance or reduce the cellular uptake of CpG, we believe that C-agarose might promote CpG transfer into Siglec-1^{+} macrophages via Siglec-1-mediated endocytosis.

CpG Treatment Activated Siglec-1^{+} Macrophages and Enhanced the Tumoricidal Effect of Lymph Node Cells

To examine the influence of CpG stimulation on Siglec-1^{+} macrophages and the subsequent composition of lymphocyte subpopulation, we performed transcriptome sequencing to elucidate the mRNA expression profiles of CpG-activated Siglec-1^{+} macrophages. The cytokine genes whose mRNAs were differentially expressed were selected and shown in Figure 2A. The ELISA results demonstrated that interferon-γ (IFN-γ), interleukin-10 (IL-10), chemokine (C-X-C motif) ligand 4 (CXCL4), and chemokine (C-C motif) ligand 5 (CCL5) could not be detected or were unchanged in the supernatant from Siglec-1^{+} macrophages, while IL-1α, IL-1β, CXCL9, CXCL10, and TNF-α showed the same change trends as those observes in the transcriptome sequencing data (Figure 2B). We also examined the mRNA level of classical macrophage phenotype markers (M1, *Tnf-α*, *Nos2*, *Mhc II*; M2, *Arg1*, *Mgl1*, *Mgl2*, and *Ym1*) in Siglec-1^{+} macrophages with CpG treatment. Lipo+CpG transfection significantly increased the mRNA level of *Tnf-α*, *Nos2*, and *Mhc II*, but showed no influence on the mRNA level of M2 markers (*Arg1*, *Mgl1*, *Mgl2*, and *Ym1*) (Figure S4).

Lymph node cells were co-cultured with Siglec-1^{+} macrophages with different treatments. Flow cytometry analysis demonstrated that CpG-treated Siglec-1^{+} macrophages could increase the ratio of CD4^{+} T cells, CD8^{+} T cells (CTLs), dendritic cells (DCs; CD11c^{+} cells), and NK cells (CD49b^{+} cells) but showed no influence on the proportion of macrophages (F4/80^{+} cells) and B cells (B220^{+} cells) (Figures 2C and 2D). Moreover, cytokine levels of IL-2, IFN-γ, and granzyme B were significantly increased in the supernatant from co-culture system containing CpG-treated Siglec-1^{+} macrophages and lymph node cells (Figure 2E). As IL-2, IFN-γ, and granzyme B could not be detected in the supernatant from CpG-treated Siglec-1^{+} macrophage alone (Figure 2B), the cytokines (IL-2, IFN-γ, and granzyme B) in the co-culture system may be secreted by lymph node cells rather than Siglec-1^{+} macrophages. As there was no significant difference between the viability of lymph node cells treated with the medium from Lipo+CpG-transfected Siglec-1^{+} macrophages and that of lymph node cells treated with the medium from Lipo+m-ODN (mismatched oligodeoxynucleotide)-transfected Siglec-1^{+} macrophages (Figure S5), the co-culture experiments indicated that lymph node cells activated by CpG-treated Siglec-1^{+} macrophages could effectively decrease the viabilities of 4T1 and B16F10 tumor cells (Figure 2F).
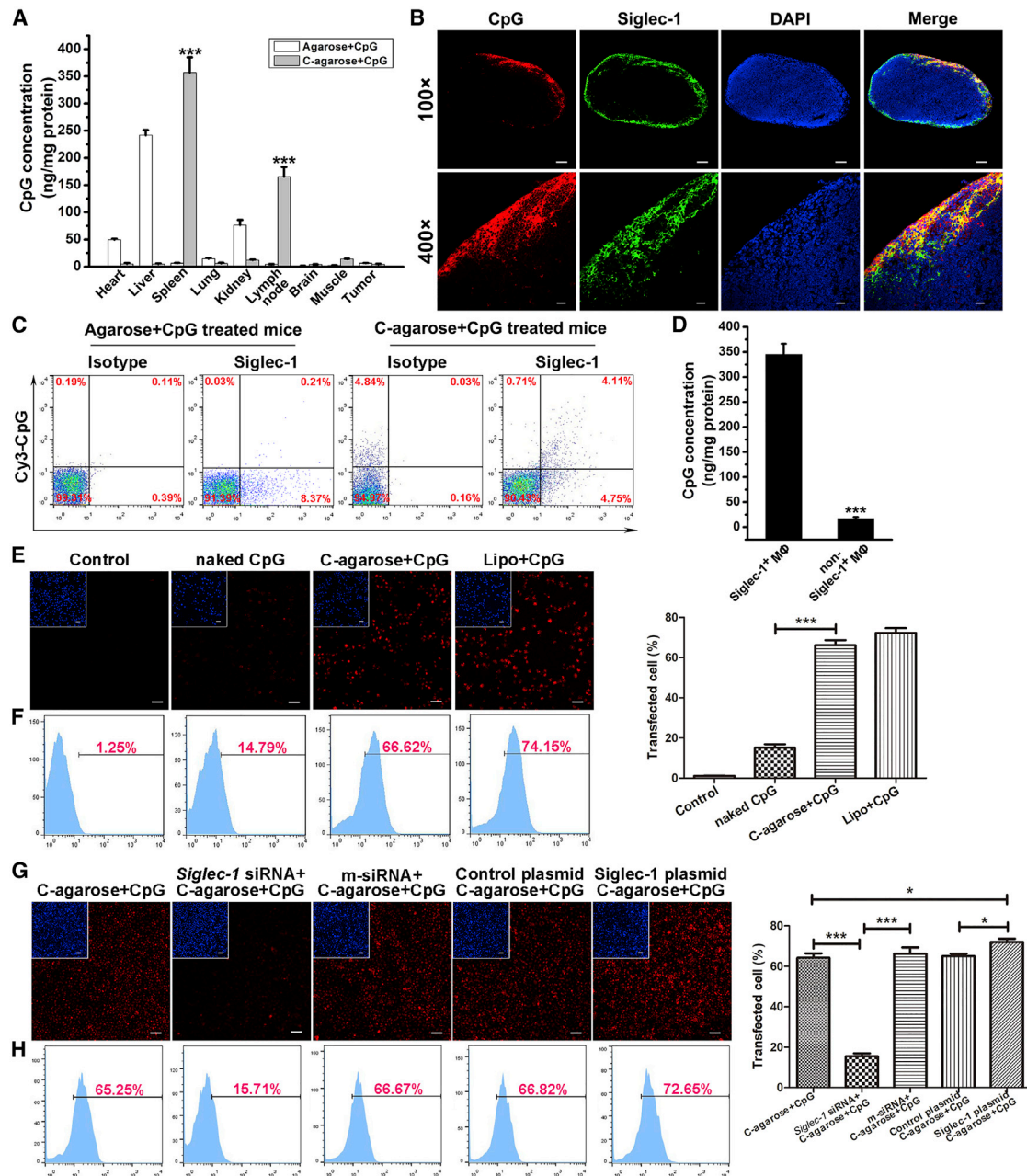
Figure 1. Biodistribution of CpG by C-agarose Gel and Cell Transfection Assay

(A) The levels of CpG in different organs from 4T1 tumor-bearing mice were examined 1 week after naked agarose+Cy3-CpG or C-agarose+Cy3-CpG gel administration. (B) Frozen sections of TDLN from tumor-bearing mice treated with C-agarose+Cy3-CpG gel implantation were stained with a Siglec-1 antibody (red, Cy3-CpG; green, Siglec-1; blue, DAPI nuclear staining). Scale bar, 100 μm for 100× or 20 μm for 400×. (C) Lymph node cells from tumor-bearing mice treated with agarose+Cy3-CpG or C-agarose+Cy3-CpG were examined by flow cytometry. (D) The levels of CpG in Siglec-1$^+$ macrophages and Siglec-1$^-$ cells were quantified by fluorescence intensity. (E and F) In vitro results of C-agarose+CpG transfection into lymph node sinus macrophages were examined by confocal microscopy (E) and quantified by a flow cytometer (F). Siglec1 siRNA, mismatched siRNA (m-siRNA), control plasmid, or Siglec-1 plasmid was transfected into Siglec-1$^+$ macrophages via Lipofectamine 2000 48 h before the addition of C-agarose+Cy3-CpG complex. Fluorescence images (G) and flow cytometry (H) results of above treated Siglec-1$^+$ macrophages (G and H) (red, Cy3-CpG; blue, DAPI nuclear staining). Scale bar, 100 μm (E and G). n = 10 mice per group. Data are representative results from five independent experiments and are expressed as the mean ± SEM. *p < 0.05, **p < 0.01, and ***p < 0.001. Lipo, Lipofectamine 2000; MΦ, macrophages; TDLN, tumor-draining lymph node.
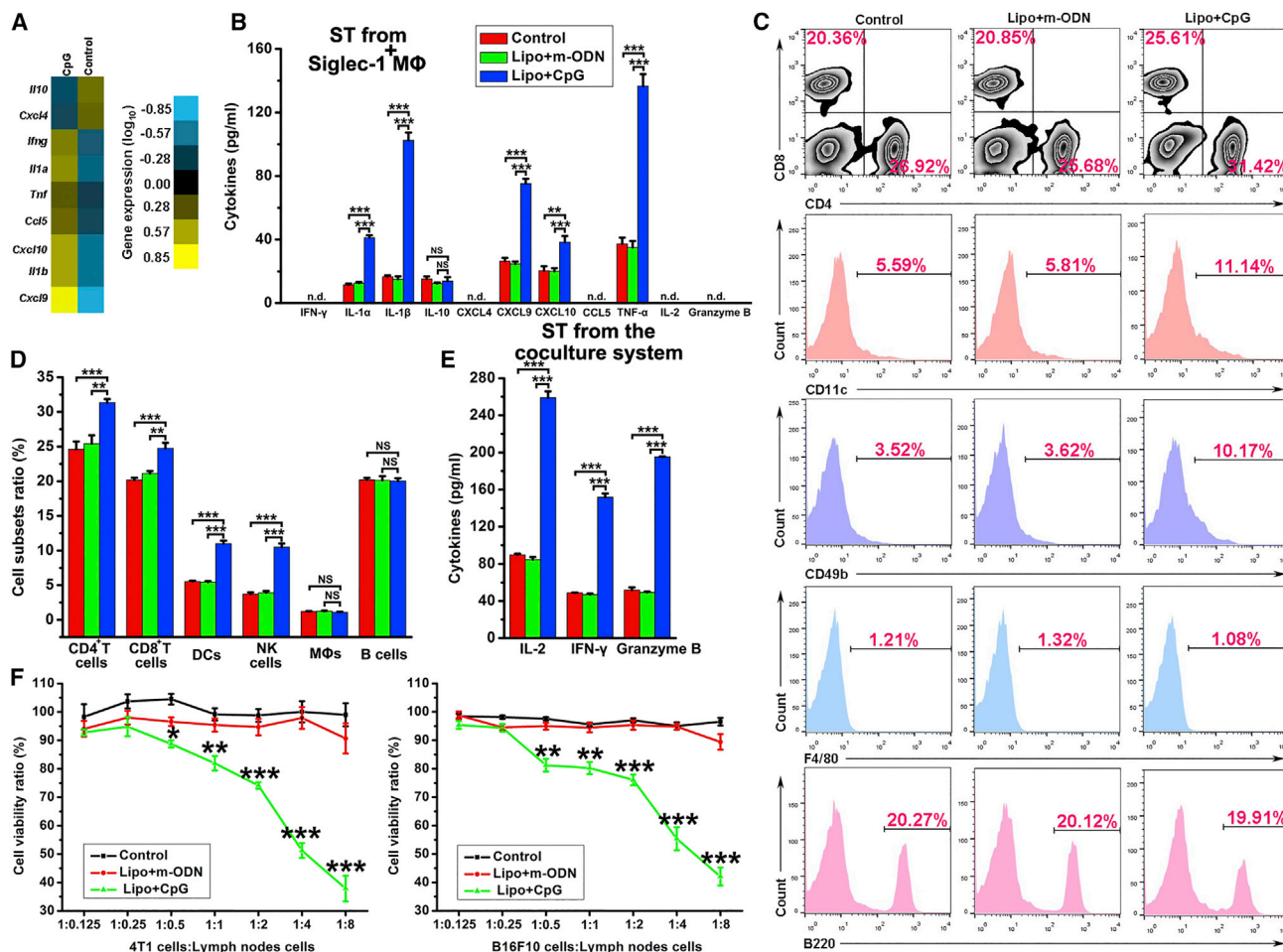
Figure 2. CpG Treatment Led to the Activation of Lymph Node Sinus Macrophages and Enhanced the Ability of Tumor-Killing Cells in Lymph Nodes

(A) The heatmap of the differentially expressed cytokines between the control group and CpG-treated group is shown. (B) Levels of cytokines (IFN-γ, IL-1α, IL-1β, IL-10, CXCL4, CXCL9, CXCL10, CCL5, TNF-α, IL-2, and granzyme B) were examined in the supernatant from lymph node sinus macrophages treated with CpG or mismatched oligonucleotide (m-ODN). (C) Flow cytometry was performed to examine the ratio of lymph node cells after co-culture with CpG-treated lymph node sinus macrophages and (D) the data was quantified. (E) Cytokine levels were examined in the supernatant from the co-culture system containing lymph node cells and CpG-treated lymph node sinus macrophages. The abilities of lymph node cells from the above-mentioned co-culture system to kill 4T1 cells and B16F10 tumor cells were examined by a CCK8 assay. n = 10 mice per group. Data are representative results from five independent experiments and are expressed as the mean ± SEM. *p < 0.05, **p < 0.01, and ***p < 0.001 (B and D); *p < 0.05, **p < 0.01, and ***p < 0.001 compared to the control (F). MΦ, macrophage; ST, supernatant; NS, not significant; n.d., not detected.

C-agarose+CpG Treatment Suppressed Both Tumor Growth and Metastasis

As CpG-pretreated lymph node cells could inhibit tumor cell growth *in vitro*, the antitumor ability of C-agarose+CpG was evaluated in both 4T1 and B16F10 tumor models. Subcutaneous injection of C-agarose+CpG hydrogel could inhibit lymph metastasis and reduce the number of lung metastatic nodules in both tumor models based on macroscopic observations (Figures 3A, 3B, 4A, and 4B) and histopathological examination (Figures 3D, 3E, 4D, and 4E). Interestingly, implantation of C-agarose+CpG hydrogel could also reduce the tumor size and weight (Figures 3B, 3C, 4B, and 4C). Survival analysis revealed that C-agarose+CpG hydrogel treatment prolonged

the lifespans of both 4T1 and B16F10 tumor-bearing mice (Figures 3F and 4F).

The Stimulating Effect of C-agarose+CpG Hydrogel on TDLN Environment

To better understand how immune cells localized in TDLN play a role in inhibiting tumor metastasis, we also examined the cell population and cytokine expression profiles in lymph nodes from tumor-bearing mice with different treatments. As shown in Figures 5A, 5B, 6A, and 6B, the proportion of CD4+ T cells, CD8+ T cells (CTLs), DCs (CD11c+ cells), and NK cells (CD49b+ cells) in lymph nodes from mice administered C-agarose+CpG treatment were significantly
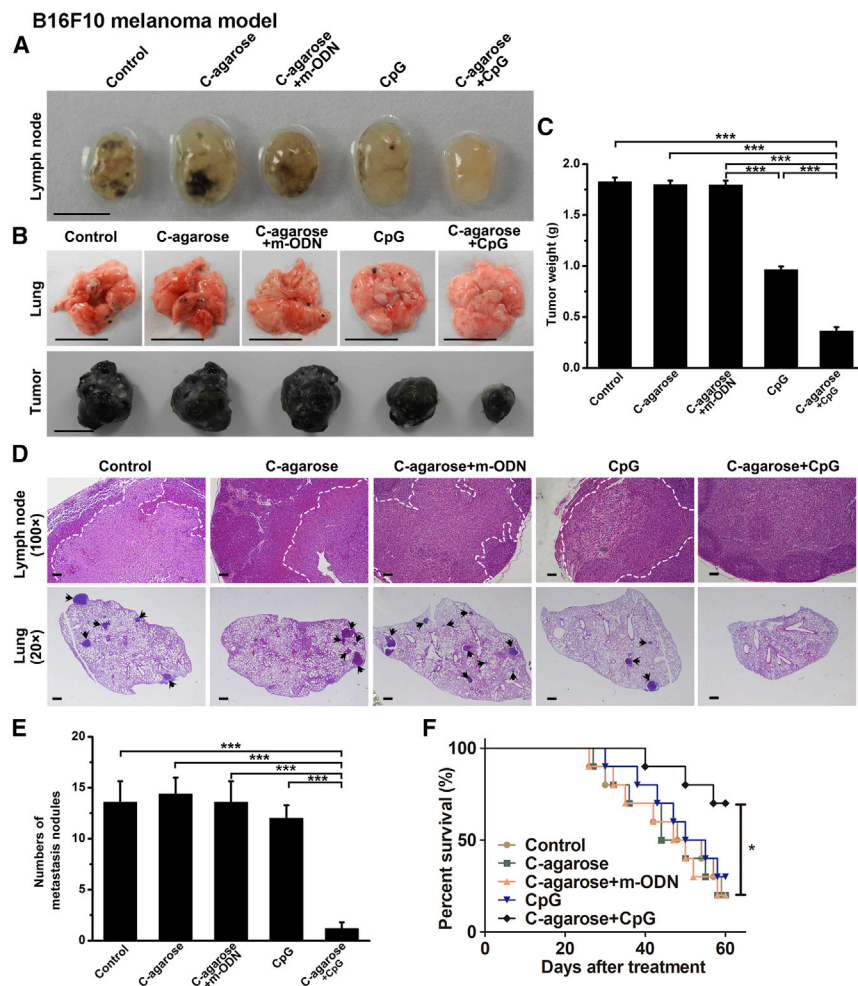
4T1 breast cancer model
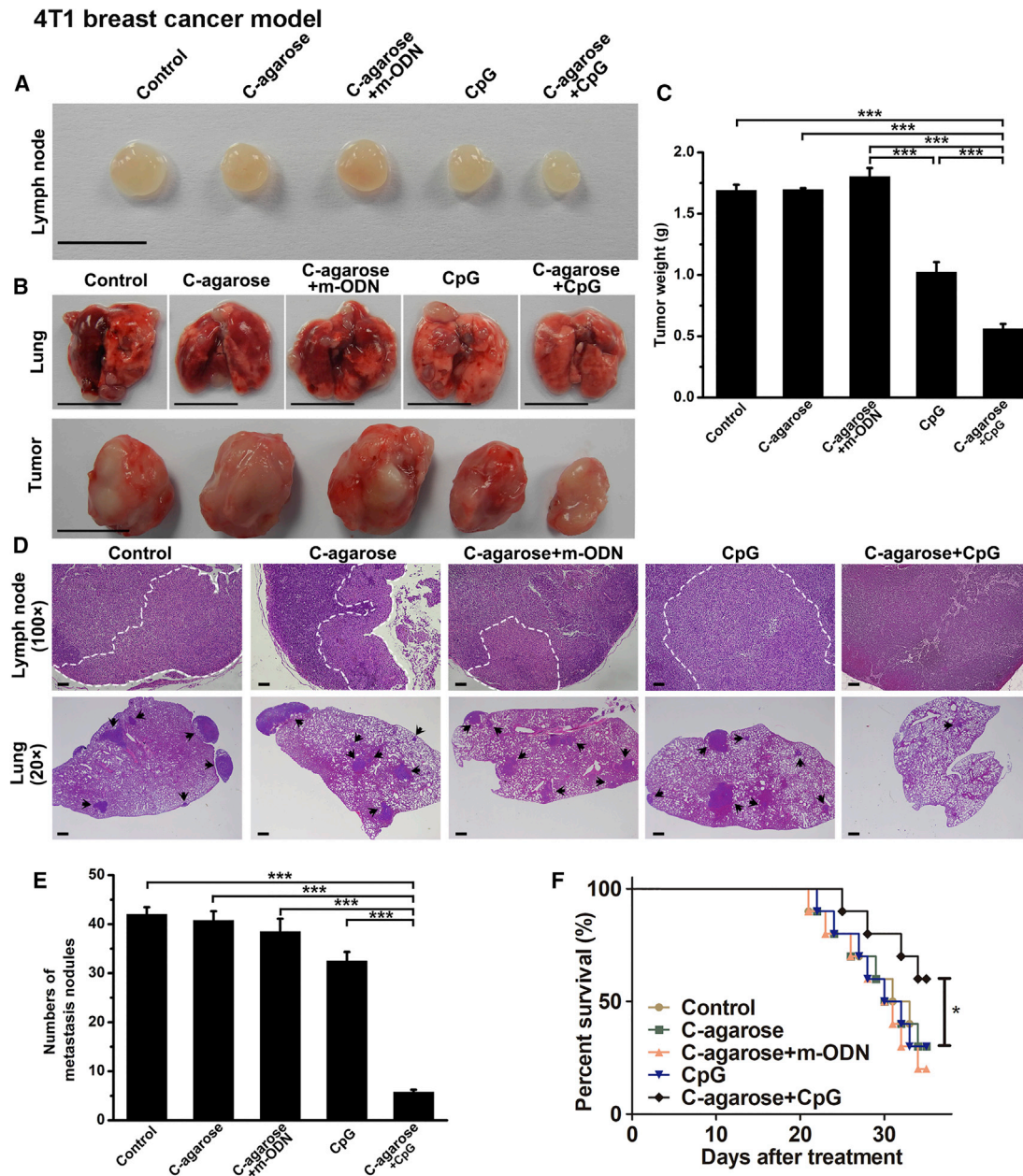
Figure 3. Antitumor Effects of C-agarose+CpG on a Murine 4T1 Breast Cancer Model

(A and B) Representative images of (A) TDLN, (B) lungs, and tumors excised from 4T1 tumor-bearing mice administered different treatments. Scale bar, 0.5 cm for (A) or 1 cm for (B). (C) The isolated tumors from mice were weighed. (D) Lymph node (100×; scale bar, 100 μm) and lung (20×; scale bar, 500 μm) sections from mice administered different treatments were stained with H&E. (E) Numbers of tumor nodules in the lung tissues from tumor-bearing mice. (F) Survival curves of tumor-bearing mice under different treatments at 35 days after model establishment. n = 10 mice per group. Data are representative results from five independent experiments and are expressed as the mean ± SEM. *p < 0.05, **p < 0.01, and ***p < 0.001 (C and E); *p < 0.05 compared to the control (F). m-ODN, mismatched oligonucleotide; TDLN, tumor-draining lymph node.

increased, whereas the percentages of macrophages and B cells was not significant changed (Figures S6 and S7). Furthermore, cytokines from TDLN, including IL-1α, IL-1β, TNF-α, CXCL9, CXCL10, IL-2, IFN-γ, and granzyme B, which may be responsible for activating lymph node cells or killing tumor cells were increased in mice treated with C-agarose+CpG (Figures 5C and 6C).

Splenectomy Showed No Influence on the Antitumor Growth or Metastatic Activity of C-agarose+CpG Hydrogel

As CpG mainly accumulated in the spleen and lymph nodes, we performed splenectomy to evaluate the potential role of the spleen in C-agarose+CpG hydrogel-mediated antitumor activity. C-agarose+CpG treatment could inhibit lymph node and lung

B16F10 melanoma model

metastasis (Figures 7A–7C and 7E), suppress tumor growth (Figures 7B and 7D), and prolong the life cycle of tumor-bearing mice (Figure 7F) in both shame-operated and splenectomized mice. As shown in Figures 7A–7F, no significant improvement or exacerbation was observed in splenectomized mice following C-agarose+CpG hydrogel treatment.
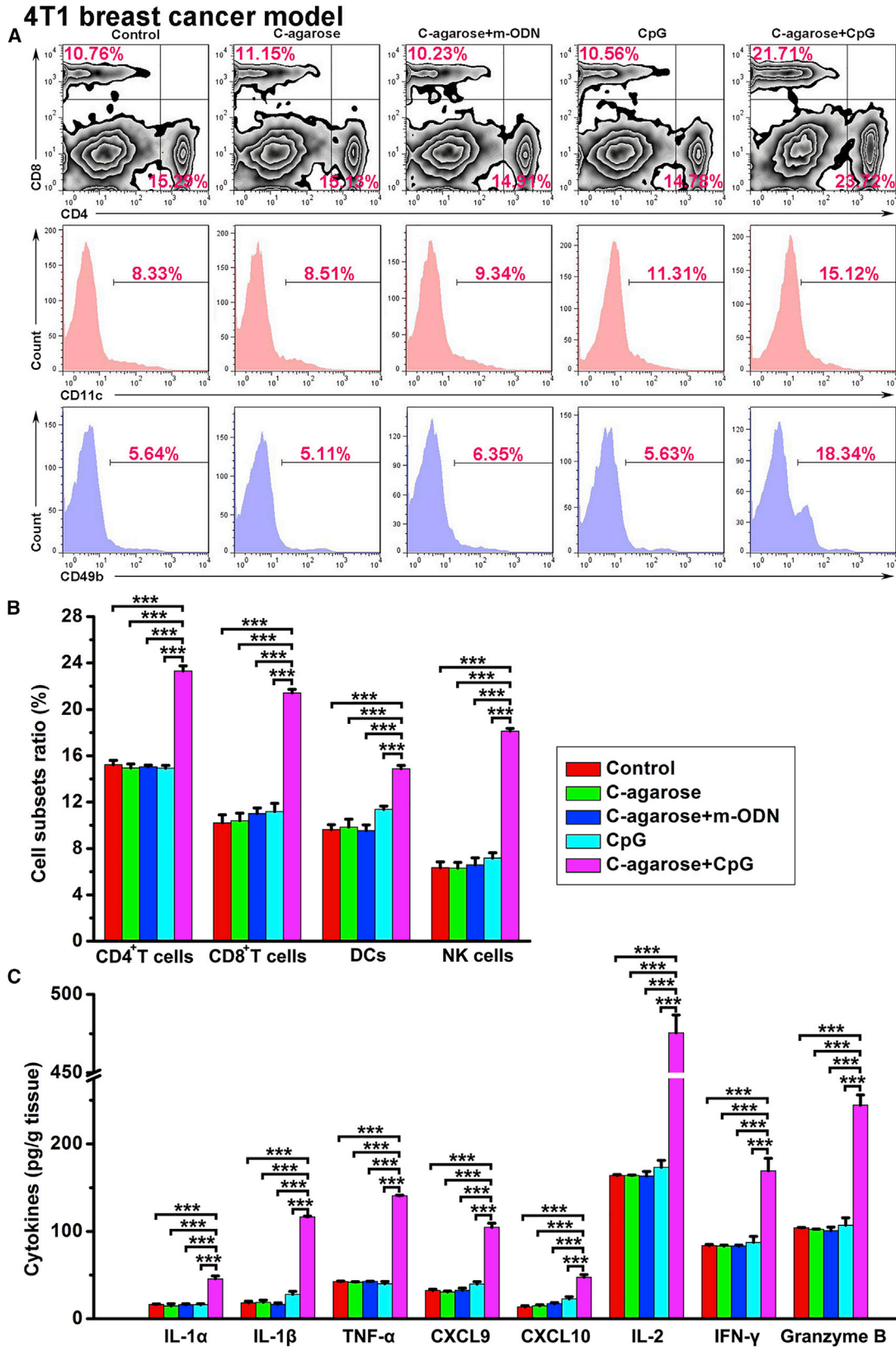
DISCUSSION

In this study, we applied a C-agarose hydrogel to deliver a CpG oligonucleotide to lymph node sinus macrophages to reverse the immune tolerance state in the TDLN, which ultimately led to the inhibition of tumor metastasis and growth.
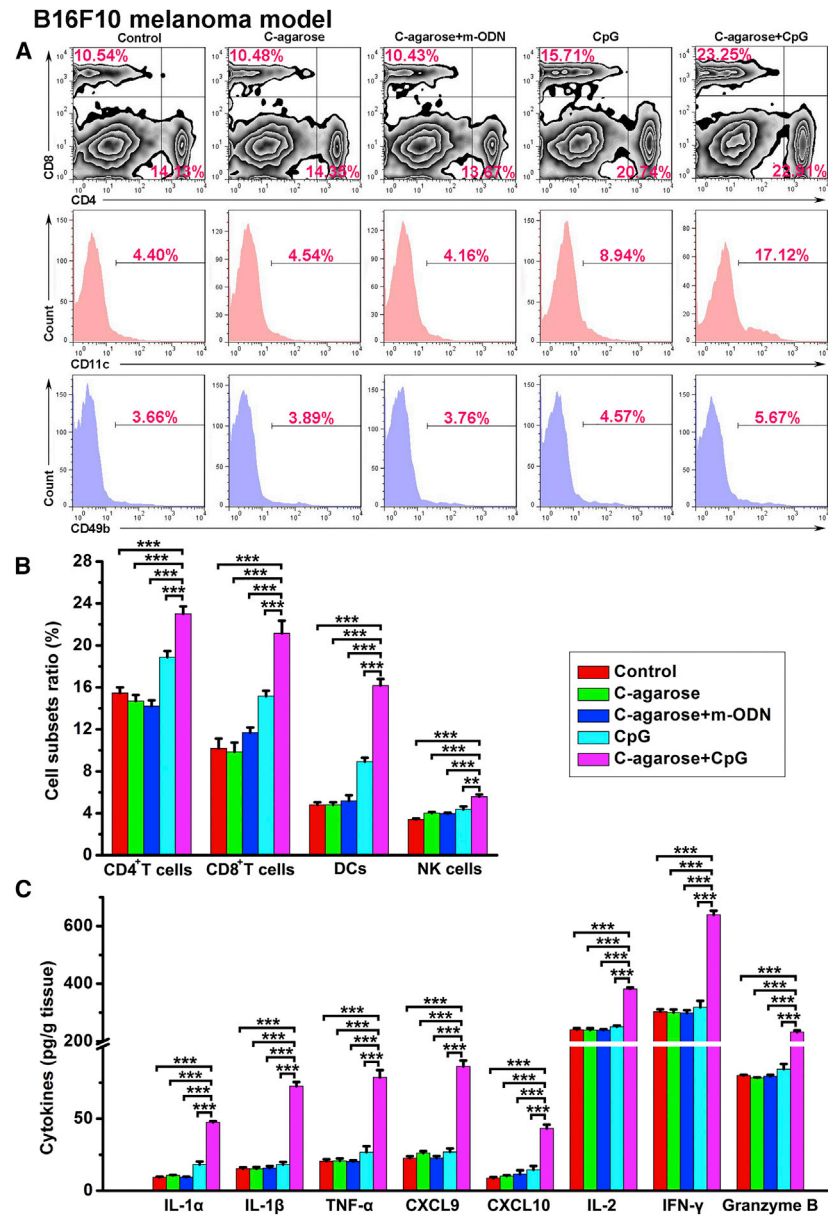
We demonstrated that subcutaneous injection of C-agarose+CpG led to the accumulation of CpG in splenic marginal zone regional macrophages and lymph node sinus macrophages.[22] The high expression of Siglec-1 is observed in both types of macrophages. The present study also indicated that C-agarose+CpG complex preferred to enter into Siglec-1$^+$ cells rather than Siglec-1$^-$ cells. Moreover, *Siglec-1* siRNA and Siglec-1 plasmid pretransfection obviously affect C-agarose+CpG

transfection. All these evidences suggest that the Siglec-1$^+$ macrophage-targeting ability of C-agarose+CpG is closely related to the interaction between Siglec-1 and the carrier itself. Siglec-1 preferentially recognizes sialic acid linkage with glycans, including galactose.[23,24] As agarose is composed of galactose, and the positively charged C-agarose binds to the negatively charged sialic acid on the cell surface, it is possible that Siglec-1 mistakes the formed complex for glycan-linked sialic acid, which leads to the phagocytosis of the C-agarose+CpG complex. Combined with the previous data showing that the deletion of infiltrated subcutaneous macrophage around the implanted gel abolished the accumulation of oligonucleotide in Siglec-1$^+$ macrophages, we speculate that C-agarose delivered the oligonucleotide into Siglec-1$^+$ macrophages in the following way:[22] when the hydrogel was implanted subcutaneously, the surrounding tissue macrophages were recruited to the injection site, infiltrated into the gel, and phagocytized the oligonucleotide-containing gel. The immunological effect of the positively charged carrier itself and the loading CpG may activate these invaded macrophages. It has been reported that activated tissue macrophages do not die at their original location but rather migrate to nearby drainage lymph nodes.[25] In the lymph nodes, the dead tissue macrophages may release C-agarose+CpG nano-complex, which may be directly ingested by sinus macrophages or enter the circulation system and be captured by the splenic marginal zone regional macrophages due to their high affinity with C-agarose.

As a potent activator of TLR9, CpG oligonucleotides have been widely used as a cancer immunotherapeutic reagent in clinical trials.[26,27] Previous studies indicated that the combination of CpG and blockers targeting the IL-10 signaling pathway could reverse the M2-like tumor-associated macrophages (TAMs) to a classical M1

4T1 breast cancer model

(legend on next page)

B16F10 melanoma model

Figure 6. C-agarose+CpG Treatments Change the Ratio of Immune Cell Subsets and Cytokine Levels in the TDLN from a Murine B16F10 Melanoma Model

(A) Lymph node cells were stained with PE-CD4 (CD4$^+$ T cells), APC-CD8 (CD8$^+$ T cells), APC-CD11c (DCs), or PE-CD49b (NK cells) and examined by flow cytometry. (B) The ratio of CD4$^+$T cells, CD8$^+$T cells, DCs, and NK cells. (C) The homogenates of lymph node were harvested to determine the levels of IL-1α, IL-1β, TNF-α, CXCL9, CXCL10, IL-2, IFN-γ, and granzyme B by ELISA, n = 10 mice per group. Data are representative results from five independent experiments and are expressed as the mean ± SEM. *p < 0.05, **p < 0.01, and ***p < 0.001. m-ODN, mismatched oligonucleotide; TDLN, tumor-draining lymph node.

(IL-1α, IL-1β, IL-12, CXCL9, CXCL10, and TNF-α).[32–39] CpG stimulation led to the increased expression of several M1-related cytokines (IL-1α, IL-1β, CXCL9, CXCL10, and TNF-α) and mRNA levels of M1 markers (increased the mRNA level of *Tnf-α*, *Nos2*, and *Mhc II*) in lymph node sinus macrophages. However, the levels of M1-related cytokine (IL-12) and M2 markers (*Arg1*, *Mgl1*, *Mgl2*, and *Ym1*) were not changed after CpG treatment. Therefore, the activation of lymph node sinus macrophages could not be simply considered as the transition of macrophages from M2 phenotype to M1 phenotype.

Previous studies indicated that lymph node sinus macrophages could promote the proliferation and activation of different immune cells via transferring antigens to DC cells, ultimately leading to the expansion and activation of CTL and NK cells.[15,40–42] Consistent with previous reports, CpG-stimulated lymph node sinus macrophages could increase the ratio of DC cells, CTL cells, and NK cells both *in vitro* and in the lymph node from tumor-bearing mice. Moreover, these characteristic cytokines (IL-2, IFN-γ, and granzyme B) closely related to CTL and NK cells were also upregulated in the supernatant from lymphocytes co-cultured with sinus macrophages.[13,43] There may be several ways via which lymph node sinus macrophages positively affect immune cell subsets. First, CpG-treated Siglec-1$^+$ macrophages can activate lymphocytes in a classical antigen-presenting manner. Second, these upregulated cytokines (IL-1α, IL-1β, and TNF-α)

phenotype.[28,29] CpG treatment could activate TAMs and restore their ability to secrete IL-12, thus exerting tumoricidal activities against tumor cells.[19,30] SCS macrophages, a subset of lymph node sinus macrophages, are localized at the first line of incoming lymphatic fluid and are easily accessible by invading pathogens.[10,31,32] It has been demonstrated that microbe infection or immunostimulant treatment enables lymph node sinus macrophages to secrete several cytokines

Figure 5. C-agarose+CpG Treatments Change the Ratio of Immune Cell Subsets and Cytokine Levels in the TDLN from a Murine 4T1 Breast Cancer Model
(A) Lymph node cells were stained with PE-CD4 (CD4$^+$ T cells), APC-CD8 (CD8$^+$ T cells), APC-CD11c (DCs), or PE-CD49b (NK cells) and examined by flow cytometry. (B) The ratio of CD4$^+$ T cells, CD8$^+$ T cells, DCs, and NK cells. (C) The homogenates of lymph nodes were harvested to determine the levels of IL-1α, IL-1β, TNF-α, CXCL9, CXCL10, IL-2, IFN-γ, and granzyme B by ELISA. n = 10 mice per group. Data are representative results from five independent experiments and are expressed as the mean ± SEM. *p < 0.05, **p < 0.01, and ***p < 0.001. m-ODN, mismatched oligonucleotide; TDLN, tumor-draining lymph node.
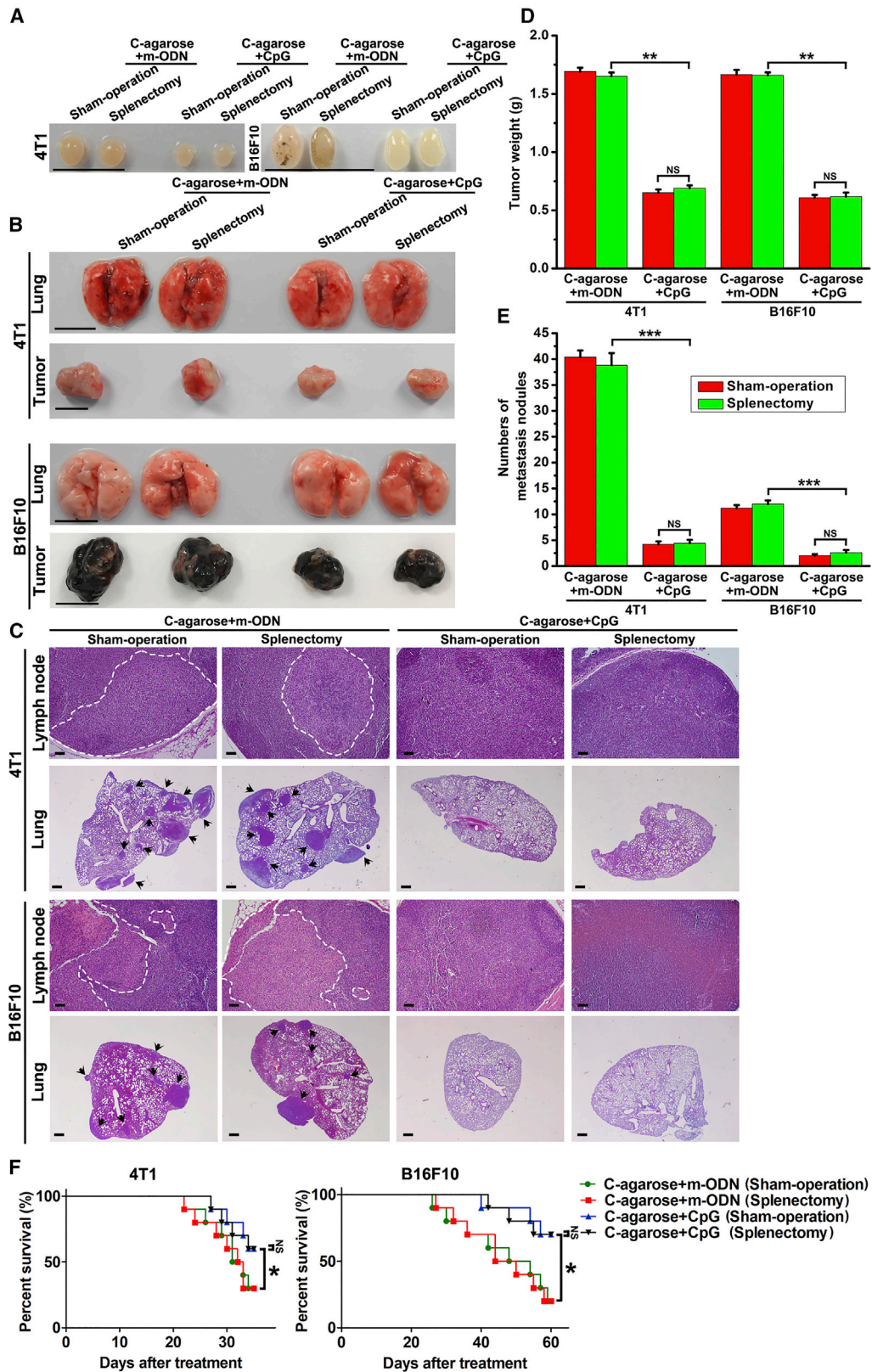
(legend on next page)

may enhance NK cells and CTL responses.[32,34] Third, CXCL9/CXCL10 can induce the migration of peripheric NK cells and CTL cells into lymph nodes.[35] Finally, Siglec-1 might function as a costimulatory molecule and activate NK cells and CTL cells via physical interaction.[44] Therefore, CpG-treated sinus macrophages induce the expansion and activation of NK cells and CTL cells and elevate the levels of tumoricidal cytokines, which generates an unviable environment for migratory tumor cells and blocks the lymphatic metastasis route. Our data confirmed that C-agarose+CpG treatment greatly decreased the metastasis size in the tumor-draining node and the number of lung metastatic nodules. Moreover, these activated immune cell subsets and related cytokines may leave the peripheral lymphoid tissue and enter the external blood, ultimately leading to the suppression of primary tumor growth. Additionally, splenectomy did not affect the antitumor growth or metastasis activity of C-agarose+CpG hydrogel. It is possible that C-agarose+CpG hydrogel-induced immune responses in lymph nodes were strong enough to suppress primary tumor growth and metastasis.

In conclusion, we herein constructed a nucleic acid drug delivery system containing C-agarose and CpG that specifically delivered CpG to lymph node sinus macrophages and generated antitumor immune responses, which prevented primary tumor growth and metastasis to distant sites. This TLR activator-based, lymph node sinus macrophage-activated therapeutic approach may be valuable for cancer immunotherapy.

MATERIALS AND METHODS
Reagents and Synthesis of Materials
The CpG 1668 oligodeoxynucleotide (5′-TCCATGACGTTCCTGATGCT-3′) and corresponding mismatch oligonucleotide (m-ODN, 5′-TCCATGAGGTTCCTGATGCT-3′), in which all nucleotides were modified with phosphorothioate, were synthesized by Thermo Fisher Scientific (Waltham, MA, USA). Cyanine 3-labeled CpG (Cy3-CpG) was used to investigate cell transfection and tissue biodistribution. Agarose (D-1 LE) was obtained from Takara Biomedical Technology (Beijing, China). N, N′-carbonyldiimidazole (CDI) and other chemical reagents were purchased from Sangon Biotech (Shanghai, China). C-agarose was synthesized by linking ethylenediamine with the hydroxyl groups of agarose using a CDI activation protocol according to a previous report.[45] The ratio of ethylenediamine introduced into the agarose was examined by elemental analysis of nitrogen (CHN-O-Rapid, Hanau, Germany), and the 5.25%-modified agarose was used for the following studies.

Preparation of C-agarose+CpG Solution and C-Agarose Hydrogel Containing CpG
Various amounts of C-agarose were completely dissolved in saline after being heated to 100°C for 15 min to obtain different concentrations of C-agarose solvent. For cell transfection, a C-agarose+CpG solution containing 1 mg/mL CpG was prepared by mixing a volume of CpG saline solution (4 mg/mL) with 3 volumes of C-agarose saline solution (4 mg/mL). For gelation *in vivo*, the C-agarose+CpG hydrogel containing 0.5 mg/mL CpG was obtained by the addition of CpG to the heated 1.5% (w/v) C-agarose solution. Then, the C-agarose solution was cooled down to 45°C and injected into tumor-bearing mice via subcutaneous administration.

Cell Isolation and Treatment
4T1 cells (a type of murine mammary carcinoma cell line, ATCC, Manassas, VA, USA) and B16F10 cells (a type of mouse melanoma cell line, ATCC) were cultured in RPMI-1640 medium and DMEM medium (Thermo Fisher Scientific) containing 10% fetal calf serum (FCS), respectively. To isolate Siglec-1^{+} macrophages, lymph nodes were isolated from mice and used to prepare a single-cell suspension. Siglec-1^{+} macrophages were collected from the single-cell suspension using a PE-labeled anti-Siglec-1 antibody and anti-PE microbeads (Miltenyi Biotec, Bergisch Gladbach, Germany). Flow cytometry analysis and trypan blue staining indicated that both the purity and viability of Siglec-1^{+} macrophages were higher than 90%.

Siglec-1[+] macrophages were seeded in 6-well plates and cultured in RPMI-1640 medium (Thermo Fisher Scientific) with 10% FCS before treatments. Then, the culture medium was removed, and Siglec-1^{+} macrophages were washed once with PBS. Next, 1 mL of Opti-MEM containing 4 μg of naked Cy3-CpG or C-agarose+CpG complex (also containing 4 μg of Cy3-CpG) was added to the wells to incubate at 37°C for 6 h. Lipofectamine 2000 was used as a positive control reagent. To examine the role of Siglec-1 in the cellular uptake of the C-agarose+CpG complex in Siglec-1^{+} macrophages, 100 pmol siRNAs targeting *Siglec-1* or corresponding control siRNAs (mismatched siRNA [m-siRNA]), control plasmid, or 4 μg Siglec-1 plasmid (vector, pECMV-MCS-FLAG; Fenghui Bio, Changsha, China) were transfected into Siglec-1^{+} macrophages 48 h before the incubation with C-agarose+CpG complex. The siRNA sequences are shown in Table S1. The expression level of Siglec-1 in macrophages treated with siRNA or plasmid was examined by western blot 48 h after transfection. Moreover, a Siglec-1 antibody (#MCA884, Bio-Rad, 10 μg/mL) was incubated with Siglec-1^{+} macrophages for 12 h before

---

Figure 7. Influence of Splenectomy on the Antitumor Activity of C-agarose+CpG

(A and B) After a sham operation or splenectomy, mice were inoculated with tumor cells and then subcutaneously injected with C-agarose+m-ODN gel or C-agarose+CpG gel. Representative images of (A) TDLN, (B) lungs, and tumors from 4T1 or B16F10 tumor-bearing mice administered different treatments are shown. Scale bar, 1 cm. (C) Lymph node (100×; scale bar, 100 μm) and lung (20×; scale bar, 500 μm) sections from tumor-bearing mice administered different treatments were stained with H&E. (D) The isolated tumors from mice were weighed. (E) Numbers of tumor nodules in the lung tissues from tumor-bearing mice. (F) Survival curves of tumor-bearing mice under different treatments at 35 days (4T1 breast cancer model) or 60 days (B16F10 melanoma model) after model establishment. *p < 0.05, **p < 0.01, and ***p < 0.001 (D and E); *p < 0.05 (the comparison between splenectomized mice with C-agarose+CpG treatment and splenectomized mice with C-agarose+m-ODN treatment); NS, not significant (the comparison between splenectomized mice with C-agarose+CpG treatment and sham-operated mice with C-agarose+CpG treatment); n = 10 mice per group. Data are representative results from five independent experiments and are expressed as the mean ± SEM. m-ODN, mismatched oligonucleotide; TDLN, tumor-draining lymph node.

the addition of C-agarose+CpG complex. The viability of Siglec-1$^+$ macrophages with different treatments was examined 48 h after transfection with siRNA or plasmid by a CCK8 kit (Dojindo Laboratories, Kumamoto, Japan). The transfection efficiency was monitored by a Nikon confocal microscope (C2$^+$, Nikon, Tokyo, Japan) and quantified by a flow cytometer (BD Biosciences, San Jose, CA, USA) 24 h after the addition of C-agarose+CpG complex.

The above differentially treated Siglec-1$^+$ macrophages were collected to extract RNA for transcriptome sequencing (Novogene Bioinformatics Technology, Beijing, China) and real-time qPCR, and the supernatant was harvested to determine the concentrations of cytokines (IFN-γ, IL-1α, IL-1β, IL-10, CXCL4, CXCL9, CXCL10, CCL5, TNF-α, IL-2, and granzyme B) using ELISA kits 24 h after transfection (R&D Systems, Minneapolis, MN, USA). Moreover, a $5*10^6$ lymph node single-cell suspension was added to wells containing $1*10^6$ CpG-treated Siglec-1$^+$ macrophages 24 h after transfection. After 4 days of co-culture, the supernatant was harvested to examine the level of cytokines (IL-2, IFN-γ, and granzyme B), and the suspended lymph node single-cell suspension was collected for flow cytometry analysis. The viability of lymph node cells with different treatment was determined by a CCK8 kit. Cell co-culture experiments were applied to examine the tumoricidal activity of activated lymph node cells. In brief, 10^4 4T1 cells or B16F10 cells in 100 μL of culture medium were co-cultured with a different number of the above mentioned-stimulated lymph node cells in 96-well plates for 24 h. A CCK8 kit was utilized to determine the viability of tumor cells. The viability of tumor cells with different treatments was calculated according to the following formula: Cell viability (%) = ([As − Al]/[Ac − Ab])*100% (As, sample absorbance of the co-culture system containing various number of lymph node cells and tumor cells; Al, sample absorbance of the culture system containing corresponding number of lymph node cells with different treatment; Ac, sample absorbance of the culture system containing corresponding number of tumor cells without any treatment; Ab, sample absorbance of the culture medium).

Tumor Model Establishment and Treatment

Female BALB/c and C57BL/6J mice (8 weeks old) with the same background were obtained from the Experimental Animal Center of Nanjing Medical School (Nanjing, China). Experimental mice were housed in a specific pathogen-free (SPF) environment in a ventilated, temperature-controlled room (23°C) with a 12 h light/12 h dark cycle. All animal procedures were performed in accordance with the Guidance Suggestions for the Care and Use of Laboratory Animals, formulated by the Ministry of Science and Technology of China, and approved by the Animal Care Ethics Committee of Nanjing University. Mice received a sham operation or a splenectomy according to a previous report 1 week prior to tumor cell implantation.[46]

4T1 cells (1×10^7 cells/mL, 100 μL) were injected into the abdominal mammary gland of normal, sham-operated, or splenectomized BALB/c mice to construct a mouse breast cancer model, and

B16F10 cells (5×10^6 cells/mL, 20 μL) were injected subcutaneously into the soles of normal, sham-operated, or splenectomized C57BL/6J mice to establish a murine melanoma cancer model. C-agarose gel containing CpG (5 mg CpG/kg body weight) was injected subcutaneously into the area near the tumor site every week from week 1 to week 3 in 4T1 tumor-bearing mice or from week 1 to week 6 in B16F10 tumor-bearing mice after tumor implantation. Mice treated with saline were used as a control, and mice infected with naked CpG, C-agarose, and C-agarose+m-ODN were used for therapeutic effect comparison. 4T1 tumor-bearing mice were sacrificed on day 25, and B16F10 tumor-bearing mice were sacrificed on day 45; their tumors were harvested for macroscopic observation and weight analysis. For survival analysis, 4T1 tumor-bearing mice were killed on day 35, and B16F10 tumor-bearing mice were sacrificed on day 60. Inguinal lymph node in 4T1 tumor-bearing mice and popliteal lymph node in B16F10 tumor-bearing mice on the side of tumor were excised as TDLNs. TDLNs and lungs in both tumor models were excised and subjected to macroscopic observation and histopathological examination. Lymph nodes were used for further flow cytometry analysis and cytokine determination.

Tissue-Distribution Assay for CpG

Agarose or C-agarose hydrogel containing Cy3-CpG at the volume of 200 μL were injected into 4T1 tumor-bearing mice subcutaneously at a dose of 5 mg CpG/kg body weight. Mice were sacrificed 1 week after gel implantation and various organs, including the heart, liver, spleen, lung, kidney, lymph node, brain, and muscle near the injection site, and the tumors were harvested. Siglec-1$^+$ macrophages were isolated by magnetic beads, and other cells collected during the isolation process were used as non-Siglec-1$^+$ macrophages. Cy3-CpG in different tissues and cells was extracted according to a previous report, and the amount was quantified via examining the fluorescence degree at 568 nm.[47] To assay the cellular localization of CpG, lymph nodes were frozen, sectioned, and incubated with a primary rat anti-mouse Siglec-1 (#MCA884, Bio-Rad, 1:200), CD3 (#ab56313, Abcam, 1:100), CD4 (#100425, Biolegend, 1:50), CD8 (#100801, Biolegend, 1:50), B220 (#103225, Biolegend, 1:50), CD11c (#97585, Cell Signaling Technology, 1:200), or CD49b (#108902, Biolegend, 1:50) antibody followed by a secondary donkey anti-rat Alexa 488 antibody (# A-21208, Thermo Fisher, 1 μg/mL) or donkey anti-rabbit Alexa 488 antibody (# A-21206, Thermo Fisher, 1 μg/mL). Then, nuclei were stained with DAPI (Sigma-Aldrich, St. Louis, MO, USA), and the sections were imaged by a Nikon C2$^+$ confocal microscope.

Flow Cytometry Analysis

The lymph node single-cell suspension was blocked in 100 μL of 1% BSA for 30 min on ice, incubated with anti-Siglec-1 (#142417, Biolegend, 10 μg/mL), anti-CD3 (#100235, Biolegend, 5 μg/mL), anti-CD4 (#100411, Biolegend, 2.5 μg/mL), anti-CD8 (#100711, Biolegend, 2.5 μg/mL), anti-CD11c (#117309, Biolegend, 2.5 μg/mL), anti-CD49b (#108909, Biolegend, 2.5 μg/mL), anti-F4/80 (#123115, Biolegend, 2.5 μg/mL), and anti-B220 (#103211, Biolegend, 2.5 μg/mL) and then analyzed on a flow cytometer (BD Biosciences).

Western Blotting Assay

Proteins extracted from cell lysate were separated with SDS-PAGE (10% polyacrylamide gels) and then transferred onto the polyvinylidine difluoride (PVDF) membranes. The membranes were blocked by 5% skimmed milk (room temperature; 1 h) and then incubated with glyceraldehyde-3-phosphate dehydrogenase (GAPDH) antibody (ab8245, Abcam, 1:10,000) and mouse Siglec-1 antibody (#MAB5610, R&D Systems, 1 μg/mL) (4°C; overnight); the membrane was incubated with anti-rat immunoglobulin G (IgG), horseradish peroxidase (HRP)-linked antibody (#7077, Cell Signaling Technology, 1:1,000) at room temperature (1 h). After rinsing with PBST (PBS with 0.1% Tween-20) five times, positive signals were detected using Super-SignalWest Pico PLUS chemiluminescent substrate (Thermo Fisher Scientific, USA) and scanned using a Tanon 4200SF chemiluminescent imaging system (Tanon, Shanghai, China).

mRNA Quantification

Quantitative real-time PCR was carried out on a 7300 sequence detection system (Applied Biosystems) with LightCyclerFastStart DNA Master SYBR Green I (Roche Diagnostics, Indianapolis, IN, USA) to examine the mRNA levels, according to the protocol provided by the manufacturer. β-actin was used as internal control for gene mRNA levels. The gene qRT-PCR primers were synthesized by Life Technologies, and the primer sequences are shown in Table S1.

Statistical Analysis

Results are expressed as the mean ± SEM. Data were statistically analyzed using Prism software (GraphPad Software, La Jolla, CA, USA) and assessed for normality or homogeneity of variance. Significant differences between two groups were evaluated by two-tailed Student's t test. Differences between multiple groups were compared using one-way ANOVA with Dunnett's tests or, if appropriate, using one-way ANOVA with post-hoc Bonferroni correction. The survival curves were analyzed by the Kaplan-Meyer log-rank test. The difference was considered significant when $p < 0.05$; NS, not significant.

SUPPLEMENTAL INFORMATION

Supplemental Information can be found online at https://doi.org/10.1016/j.omtn.2019.04.016.

AUTHOR CONTRIBUTIONS

L.D., Z.H., and J.Z. designed the study; J.H., J.X., M.L., Y.Z., and H.Y. performed the experiments and analyzed the data; J.H. and Z.H. wrote the manuscript; and L.D. and J.C. revised the manuscript. All authors read and approved the final manuscript.

CONFLICTS OF INTEREST

The authors declare no competing interests.

ACKNOWLEDGMENTS

REFERENCES

1. Cochran, A.J., Huang, R.R., Lee, J., Itakura, E., Leong, S.P., and Essner, R. (2006). Tumour-induced immune modulation of sentinel lymph nodes. Nat. Rev. Immunol. 6, 659–670.

2. Karaman, S., and Detmar, M. (2014). Mechanisms of lymphatic metastasis. J. Clin. Invest. 124, 922–928.

3. Ran, S., Volk, L., Hall, K., and Flister, M.J. (2010). Lymphangiogenesis and lymphatic metastasis in breast cancer. Pathophysiology 17, 229–251.

4. White, R.R., Stanley, W.E., Johnson, J.L., Tyler, D.S., and Seigler, H.F. (2002). Long-term survival in 2,505 patients with melanoma with regional lymph node metastasis. Ann. Surg. 235, 879–887.

5. Chandrasekaran, S., Chan, M.F., Li, J., and King, M.R. (2016). Super natural killer cells that target metastases in the tumor draining lymph nodes. Biomaterials 77, 66–76.

6. Lee, J.H., Torisu-Itakara, H., Cochran, A.J., Kadison, A., Huynh, Y., Morton, D.L., and Essner, R. (2005). Quantitative analysis of melanoma-induced cytokine-mediated immunosuppression in melanoma sentinel nodes. Clin. Cancer Res. 11, 107–112.

7. van Dongen, J.A., Voogd, A.C., Fentiman, I.S., Legrand, C., Sylvester, R.J., Tong, D., van der Schueren, E., Helle, P.A., van Zijl, K., and Bartelink, H. (2000). Long-term results of a randomized trial comparing breast-conserving therapy with mastectomy: European Organization for Research and Treatment of Cancer 10801 trial. J. Natl. Cancer Inst. 92, 1143–1150.

8. Wada, N., Duh, Q.Y., Sugino, K., Iwasaki, H., Kameyama, K., Mimura, T., Ito, K., Takami, H., and Takanashi, Y. (2003). Lymph node metastasis from 259 papillary thyroid microcarcinomas: frequency, pattern of occurrence and recurrence, and optimal strategy for neck dissection. Ann. Surg. 237, 399–407.

9. Minchinton, A.I., and Tannock, I.F. (2006). Drug penetration in solid tumours. Nat. Rev. Cancer 6, 583–592.

10. Jones, D., Pereira, E.R., and Padera, T.P. (2018). Growth and Immune Evasion of Lymph Node Metastasis. Front. Oncol. 8, 36.

11. Robbins, P.D., and Morelli, A.E. (2014). Regulation of immune responses by extracellular vesicles. Nat. Rev. Immunol. 14, 195–208.

12. Shiota, T., Miyasato, Y., Ohnishi, K., Yamamoto-Ibusuki, M., Yamamoto, Y., Iwase, H., Takeya, M., and Komohara, Y. (2016). The Clinical Significance of CD169-Positive Lymph Node Macrophage in Patients with Breast Cancer. PLoS ONE 11, e0166680.

13. Garcia, Z., Lemaître, F., van Rooijen, N., Albert, M.L., Levy, Y., Schwartz, O., and Bousso, P. (2012). Subcapsular sinus macrophages promote NK cell accumulation and activation in response to lymph-borne viral particles. Blood 120, 4744–4750.

14. Chávez-Galán, L., Olleros, M.L., Vesin, D., and Garcia, I. (2015). Much More than M1 and M2 Macrophages, There are also CD169(+) and TCR(+) Macrophages. Front. Immunol. 6, 263.

15. Komohara, Y., Ohnishi, K., and Takeya, M. (2017). Possible functions of CD169-positive sinus macrophages in lymph nodes in anti-tumor immune responses. Cancer Sci. 108, 290–295.

16. Saito, Y., Ohnishi, K., Miyashita, A., Nakahara, S., Fujiwara, Y., Horlad, H., Motoshima, T., Fukushima, S., Jinnin, M., Ihn, H., et al. (2015). Prognostic Significance of CD169+ Lymph Node Sinus Macrophages in Patients with Malignant Melanoma. Cancer Immunol. Res. 3, 1356–1363.

17. Ohnishi, K., Komohara, Y., Saito, Y., Miyamoto, Y., Watanabe, M., Baba, H., and Takeya, M. (2013). CD169-positive macrophages in regional lymph nodes are associated with a favorable prognosis in patients with colorectal carcinoma. Cancer Sci. 104, 1237–1244.

18. Ohnishi, K., Yamaguchi, M., Erdenebaatar, C., Saito, F., Tashiro, H., Katabuchi, H., Takeya, M., and Komohara, Y. (2016). Prognostic significance of CD169-positive lymph node sinus macrophages in patients with endometrial carcinoma. Cancer Sci. 107, 846–852.

19. Klinman, D.M. (2004). Immunotherapeutic uses of CpG oligodeoxynucleotides. Nat. Rev. Immunol. 4, 249–258.

20. Krieg, A.M. (2006). Therapeutic potential of Toll-like receptor 9 activation. Nat. Rev. Drug Discov. 5, 471–484.

21. Heikenwalder, M., Polymenidou, M., Junt, T., Sigurdson, C., Wagner, H., Akira, S., Zinkernagel, R., and Aguzzi, A. (2004). Lymphoid follicle destruction and immuno-suppression after repeated CpG oligodeoxynucleotide administration. Nat. Med. 10, 187–192.

22. Huang, Z., Zhang, Z., Zha, Y., Liu, J., Jiang, Y., Yang, Y., Shao, J., Sun, X., Cai, X., Yin, Y., et al. (2012). The effect of targeted delivery of anti-TNF-α oligonucleotide into CD169+ macrophages on disease progression in lupus-prone MRL/lpr mice. Biomaterials 33, 7605–7612.

23. Hartnell, A., Steel, J., Turley, H., Jones, M., Jackson, D.G., and Crocker, P.R. (2001). Characterization of human sialoadhesin, a sialic acid binding receptor expressed by resident and inflammatory macrophage populations. Blood 97, 288–296.

24. O'Neill, A.S., van den Berg, T.K., and Mullen, G.E. (2013). Sialoadhesin - a macro-phage-restricted marker of immunoregulation and inflammation. Immunology 138, 198–207.

25. Bellingan, G.J., Caldwell, H., Howie, S.E., Dransfield, I., and Haslett, C. (1996). In vivo fate of the inflammatory macrophage during the resolution of inflammation: inflam-matory macrophages do not die locally, but emigrate to the draining lymph nodes. J. Immunol. 157, 2577–2585.

26. Melisi, D., Frizziero, M., Tamburrino, A., Zanotto, M., Carbone, C., Piro, G., and Tortora, G. (2014). Toll-Like Receptor 9 Agonists for Cancer Therapy. Biomedicines 2, 211–228.

27. Le Noci, V., Tortoreto, M., Gulino, A., Storti, C., Bianchi, F., Zaffaroni, N., Tripodo, C., Tagliabue, E., Balsari, A., and Sfondrini, L. (2015). Poly(I:C) and CpG-ODN com-bined aerosolization to treat lung metastases and counter the immunosuppressive microenvironment. OncoImmunology 4, e1040214.

28. Yuan, R., Li, S., Geng, H., Wang, X., Guan, Q., Li, X., Ren, C., and Yuan, X. (2017). Reversing the polarization of tumor-associated macrophages inhibits tumor metas-tasis. Int. Immunopharmacol. 49, 30–37.

29. Guiducci, C., Vicari, A.P., Sangaletti, S., Trinchieri, G., and Colombo, M.P. (2005). Redirecting in vivo elicited tumor infiltrating macrophages and dendritic cells towards tumor rejection. Cancer Res. 65, 3437–3446.

30. Pal, R., Chakraborty, B., Nath, A., Singh, L.M., Ali, M., Rahman, D.S., Ghosh, S.K., Basu, A., Bhattacharya, S., Baral, R., and Sengupta, M. (2016). Noble metal nanoparticle-induced oxidative stress modulates tumor associated macrophages (TAMs) from an M2 to M1 phenotype: An in vitro approach. Int. Immunopharmacol. 38, 332–341.

31. Junt, T., Moseman, E.A., Iannacone, M., Massberg, S., Lang, P.A., Boes, M., Fink, K., Henrickson, S.E., Shayakhmetov, D.M., Di Paolo, N.C., et al. (2007). Subcapsular sinus macrophages in lymph nodes clear lymph-borne viruses and present them to antiviral B cells. Nature 450, 110–114.

32. Asano, K., Nabeyama, A., Miyake, Y., Qiu, C.H., Kurita, A., Tomura, M., Kanagawa, O., Fujii, S., and Tanaka, M. (2011). CD169-positive macrophages dominate antitumor immunity by crosspresenting dead cell-associated antigens. Immunity 34, 85–95.

33. Fujiwara, Y., Saito, Y., Shiota, T., Cheng, P., Ikeda, T., Ohnishi, K., Takeya, M., and Komohara, Y. (2018). Natural compounds that regulate lymph node sinus macrophages: Inducing an anti-tumor effect by regulating macrophage activation. J. Clin. Exp. Hematop. 58, 17–23.

34. Di Paolo, N.C., Miao, E.A., Iwakura, Y., Murali-Krishna, K., Aderem, A., Flavell, R.A., Papayannopoulou, T., and Shayakhmetov, D.M. (2009). Virus binding to a plasma membrane receptor triggers interleukin-1 alpha-mediated proinflammatory macrophage response in vivo. Immunity 31, 110–121.

35. Oh, D.S., Oh, J.E., Jung, H.E., and Lee, H.K. (2017). Transient Depletion of CD169+ Cells Contributes to Impaired Early Protection and Effector CD8+ T Cell Recruitment against Mucosal Respiratory Syncytial Virus Infection. Front. Immunol. 8, 819.

36. Kastenmüller, W., Brandes, M., Wang, Z., Herz, J., Egen, J.G., and Germain, R.N. (2013). Peripheral prepositioning and local CXCL9 chemokine-mediated guidance orchestrate rapid memory CD8+ T cell responses in the lymph node. Immunity 38, 502–513.

37. Porta, C., Rimoldi, M., Raes, G., Brys, L., Ghezzi, P., Di Liberto, D., Dieli, F., Ghisletti, S., Natoli, G., De Baetselier, P., et al. (2009). Tolerance and M2 (alternative) macro-phage polarization are related processes orchestrated by p50 nuclear factor kappaB. Proc. Natl. Acad. Sci. USA 106, 14978–14983.

38. Tokunaga, R., Zhang, W., Naseem, M., Puccini, A., Berger, M.D., Soni, S., McSkane, M., Baba, H., and Lenz, H.J. (2018). CXCL9, CXCL10, CXCL11/CXCR3 axis for immune activation - A target for novel cancer therapy. Cancer Treat. Rev. 63, 40–47.

39. Wu, X., Takekoshi, T., Sullivan, A., and Hwang, S.T. (2011). Inflammation and tumor microenvironment in lymph node metastasis. Cancers (Basel) 3, 927–944.

40. Liang, R., Xie, J., Li, J., Wang, K., Liu, L., Gao, Y., Hussain, M., Shen, G., Zhu, J., and Tao, J. (2017). Liposomes-coated gold nanocages with antigens and adjuvants targeted delivery to dendritic cells for enhancing antitumor immune response. Biomaterials 149, 41–50.

41. Moalli, F., Proulx, S.T., Schwendener, R., Detmar, M., Schlapbach, C., and Stein, J.V. (2015). Intravital and whole-organ imaging reveals capture of melanoma-derived an-tigen by lymph node subcapsular macrophages leading to widespread deposition on follicular dendritic cells. Front. Immunol. 6, 114.

42. Bernhard, C.A., Ried, C., Kochanek, S., and Brocker, T. (2015). CD169+ macrophages are sufficient for priming of CTLs with specificities left out by cross-priming dendritic cells. Proc. Natl. Acad. Sci. USA 112, 5461–5466.

43. Zhang, J., Xu, J., Zhang, R.X., Zhang, Y., Ou, Q.J., Li, J.Q., Jiang, Z.Z., Wu, X.J., Fang, Y.J., and Zheng, L. (2016). CD169 identifies an activated CD8(+) T cell subset in regional lymph nodes that predicts favorable prognosis in colorectal cancer patients. OncoImmunology 5, e1177690.

44. van Dinther, D., Veninga, H., Iborra, S., Borg, E.G.F., Hoogterp, L., Olesek, K., Beijer, M.R., Schetters, S.T.T., Kalay, H., Garcia-Vallejo, J.J., et al. (2018). Functional CD169 on Macrophages Mediates Interaction with Dendritic Cells for CD8+ T Cell Cross-Priming. Cell Rep. 22, 1484–1495.

45. Dong, L., Xia, S., Chen, H., Chen, J., and Zhang, J. (2009). Spleen-specific suppression of TNF-alpha by cationic hydrogel-delivered antisense nucleotides for the prevention of arthritis in animal models. Biomaterials 30, 4416–4426.

46. Rezende, A.B., Neto, N.N., Fernandes, L.R., Ribeiro, A.C., Alvarez-Leite, J.I., and Teixeira, H.C. (2011). Splenectomy increases atherosclerotic lesions in apolipopro-tein E deficient mice. J. Surg. Res. 171, e231–e236.

47. Huang, Z., Zhang, Z., Jiang, Y., Zhang, D., Chen, J., Dong, L., and Zhang, J. (2012). Targeted delivery of oligonucleotides into tumor-associated macrophages for cancer immunotherapy. J. Control. Release 158, 286–292.